# Measurements of Emittance and Absolute Spectral Flux of the PETRA Undulator at DESY Hamburg

**U. Hahn,**[a] **H. Schulte-Schrepping,**[a] **K. Balewski,**[a] **J. R. Schneider,**[a] **P. Ilinski,**[b]
**B. Lai,**[b] **W. Yun,**[b] **D. Legnini**[b] **and E. Gluskin**[b]

[a]*Hamburger Synchrotronstrahlungslabor HASYLAB at Deutsches Elektronen-Synchrotron DESY, Notkestrasse 85, Hamburg D-22607, Germany, and* [b]*Advanced Photon Source, Argonne National Laboratory, 9700 South Cass Avenue, Argonne, Illinois 60439, USA. E-mail: hahn@desy.de*

The first synchrotron radiation beamline using a 4 m-long undulator at the 12 GeV storage ring PETRA delivers hard X-ray photons usable up to 300 keV. The photon intensity is measured on an absolute scale in the energy range between 16 and 60 keV and compared with calculated intensities. The experimental set-up described is also used to measure the horizontal and vertical emittance of the source.

**Keywords: hard X-rays; undulators; spectral flux; emittance.**

## 1. Introduction

An undulator has been recently installed at a straight section of the PETRA storage ring (Balewski, Brefeld, Hahn, Pflüger & Rossmanith, 1995). This is a 3.3 cm-period device with 121 periods that provides high-brilliance X-ray radiation in the 20–300 keV energy range (HASYLAB, 1994a).

The energy of the $n$th undulator harmonic is calculated according to

$$\varepsilon_n \ (\text{keV}) = 2.483 \times 10^{-7} n\gamma^2 / [\lambda_0 (1 + 0.5K^2)], \quad (1)$$

with $n$ representing the order of the harmonic. $\gamma$ is the energy of the stored electrons or positrons in units of the electron rest mass, $\lambda_0$ is the period of the undulator structure and $K$ represents the deflection parameter,

$$K = 0.934 \, \lambda_0 B_0, \quad (2)$$

with $B_0$ being the maximum magnetic field on the undulator axis (in T) and $\lambda_0$ is measured in cm. The operation of the storage ring at 12 GeV shifts the undulator harmonics very effectively to higher photon energies as the energy of the undulator harmonic $\varepsilon_n$ is proportional to the square of the energy of the stored electrons. This largely increases the range of tunability of the fundamental harmonic. Fig. 1 shows the spectral brightness of the PETRA undulator for a storage ring energy of 12 GeV, with the present horizontal emittance of 54 nm rad and with a possible improved emittance (15 nm rad). The spectra are compared with different sources for hard X-rays operated at the ESRF in Grenoble at a storage ring energy of 6 GeV.

The performance of the PETRA undulator was verified by measuring the absolute value of the spectral flux and comparing it with its theoretical value. This was accomplished by measuring X-rays scattered from He gas, whose

differential cross section is well known, using an energy-dispersive solid-state Si(Li) detector. The emittance of the PETRA storage ring was measured using the same set-up. Earlier versions of this experimental set-up were used to
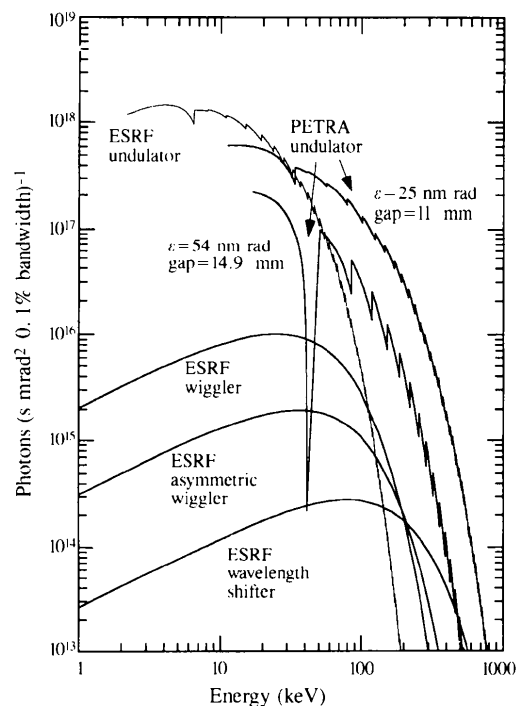


**Figure 1**
Angular flux of the PETRA undulator at 12 GeV compared with different sources of hard X-rays operated at the ESRF in Grenoble at 6 GeV (4 nm rad emittance, 1% coupling, 200 mA). The spectrum of the PETRA undulator with 54 nm rad emittance, 2% coupling and 60 mA corresponds to the present flux. The 15 nm rad spectrum shows the PETRA flux with a possible improved emittance at a reduced magnet gap of 11 mm.

measure the spectral flux of the APS/CHESS undulator (Ilinski, Yun, Lai, Gluskin & Cai, 1995; includes references to the basic technique used in this paper) and were also tested at the NSLS (unpublished results).

## 2. Experimental set-up

The PETRA storage ring was operated at 12 GeV; during the commissioning of the beamline the positron current varied between 1 and 5 mA. The experiment was performed in the first optical enclosure of the experimental hall at a distance of 105 m from the source point (HASYLAB, 1994b). An overview of the undulator beamline at PETRA is given in Fig. 2. A feedback system using the two photoemission beam-position monitors was able to stabilize the position and angle of the undulator beam to a horizontal and vertical beam stability of better than 10 μm at a distance of 106 m. The white beam was filtered by a 1 mm-thick Be front end window and a 1.13 mm-thick carbon filter to protect the window. The experimental set-up (Fig. 3) was mounted on an optical table, which has five degrees of freedom for alignment (APS design) (Barraza, Shu & Kuzay, 1994).

A water-cooled conical pinhole (entrance diameter 10 mm, exit diameter 0.8 mm, length 210 mm) was used as the first aperture in the undulator beam; it removed a substantial fraction of the total power of the beam. The pinhole was followed by a water-cooled slit system to define an undulator beam cross section of 250 × 250 μm². The slits were made of 1.4 mm-thick molybdenum blades. At 60 keV the transmission was 0.2%, at 100 keV the

transmission increased to ~30%. The distance between the slit system and the source was 106 m.

For absolute flux measurements it is necessary to know the number of He atoms that scatter X-rays into the detector aperture. The cross section of the scattering volume is defined by the width of the entrance slit. The observed length of the scattering volume is defined by an aperture slit and the sensitive area of the detector (Fig. 4). The aperture slit with 1 mm-thick tungsten blades was located 31.5 mm from the centre of the He chamber. The slit size was varied during the experiment from 1.0 to 2.5 mm for achieving a count rate <1000 counts s⁻¹ at the detector. He gas flowed continuously through the chamber, with its pressure monitored by a manometer. X-rays scattered by the He gas left the chamber through a 25 μm-thick Kapton window.

The solid-state detector with a 3.2 mm-thick Si(Li) crystal (EG&G ORTEC SLP 06165PS) and a sensitive area of 6.0 mm in diameter was located 307 mm from the centre of the He chamber. The amplifier shaping time was 6 μs.

The efficiency of a semiconductor detector is a product of the intrinsic efficiency of the sensitive volume and several correction factors (Cohen, 1980). However, transmission factors for the beryllium window, the gold layer, and the frontal dead layers, as well as escape peak correction, are negligible for the Si(Li) detector for photon energies above 10 keV.

The undulator generates high-energy X-rays with a critical energy of 48 keV at a gap of 16 mm. A 100 mm-thick tungsten block with a 5 mm-diameter hole was placed between the entrance slits and the He chamber to reduce for-
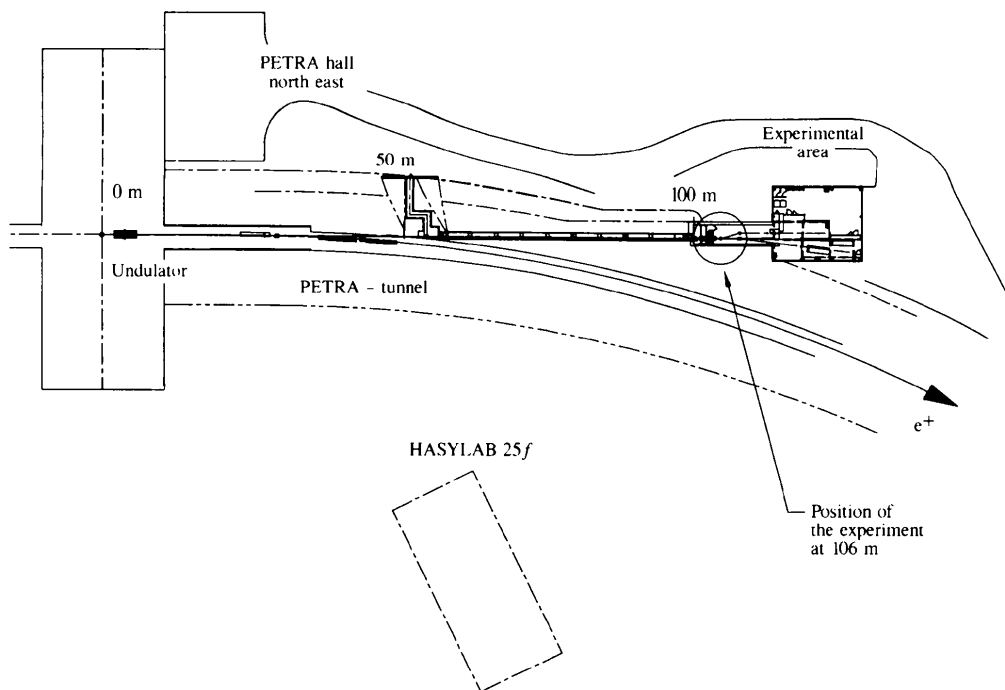


**Figure 2**
Overview of the undulator beamline at PETRA.

ward scattering, fluorescence and *bremsstrahlung* radiation. The pinhole, the entrance slits and the tungsten block were additionally shielded with lead and placed in a hutch with an He atmosphere. This hutch was connected to the upstream beamline exit Be window and to the downstream He scattering chamber (Fig. 3). The background was reduced to a negligible level with 18 mm lead shielding around the detector.

## 3. Results

The undulator spectral flux measurements were made at gap sizes of 16, 20 and 24 mm, with corresponding deflection parameters $K$ = 1.55, 1.04 and 0.7.

### 3.1. *Emittance*

The first test was to measure the source emittance to verify proper operation of the storage ring and the undulator. This was achieved by measuring the beam size by scanning the slit in the vertical and the horizontal directions and by counting only photons which come from the first undulator harmonic. Fig. 5 shows an example of a horizontal and vertical scan for an undulator gap of 20 mm. The Gaussian fits provided the standard deviations of the measured intensity distributions. In this case standard

deviations of $\sigma_m$ = 0.87 mm in the vertical and $\sigma_m$ = 4.8 mm in the horizontal were obtained.

On the other hand, the standard deviation of the measured intensity distribution for the first undulator harmonic $\sigma_m$ is calculated according to

$$\sigma_m^2 = \sigma^2 + D^2\sigma'^2 + D^2\lambda_1/2L + (a/3)^2, \tag{3}$$

where $\sigma$ is the source size, $\sigma'$ is the source divergence, $D$ is the distance to the source, $\lambda_1$ is the wavelength of the first harmonic, $L$ is the length of the undulator and $a$ is the entrance slit width (the term $a/3$ is an approximation of a square function by a Gaussian function). With $\sigma\sigma' = \varepsilon$ and $\sigma/\sigma' = \beta$, the emittance can be calculated from the beam size measurement by

$$\varepsilon = [\sigma_m^2 - D^2\lambda_1/2L - (a/3)^2]/(\beta + D^2/\beta). \tag{4}$$

Using the known value of the $\beta$-function in vertical and horizontal directions (25 m), the horizontal emittance was found to be 52 nm rad. The vertical emittance was determined to 2 nm rad, which corresponds to an emittance coupling of 3.8%. This is close to the expected values for the actual PETRA operation at 12 GeV.

After orbit corrections the vertical emittance was reduced to 1.4 nm rad, which corresponds to an emittance coupling of 3%.

### 3.2. *Spectral flux*

Figs. 6–8 show the spectral flux distributions measured at different magnetic gaps of the undulator. For the 20 mm gap (Fig. 7) an additional measurement with the improved vertical emittance is also shown. The measured flux is compared with the theoretical on-axis flux calculated for an ideal undulator with sinusoidal fields, for vertical emit-
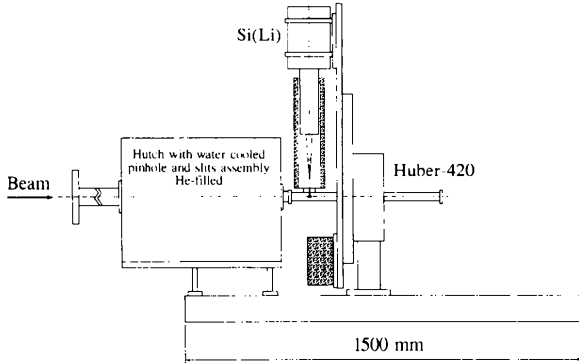


**Figure 3**
Experimental set-up (side view). The entrance water-cooled slits were placed at a distance of 106 m from the undulator centre.
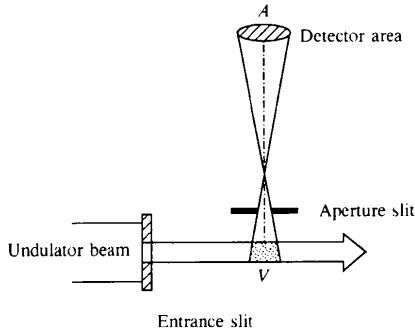


**Figure 4**
The detectable scattering volume, $V$, defined by the area of the entrance slits, the aperture slit and the sensitive area of the Si(Li) detector, $A$.
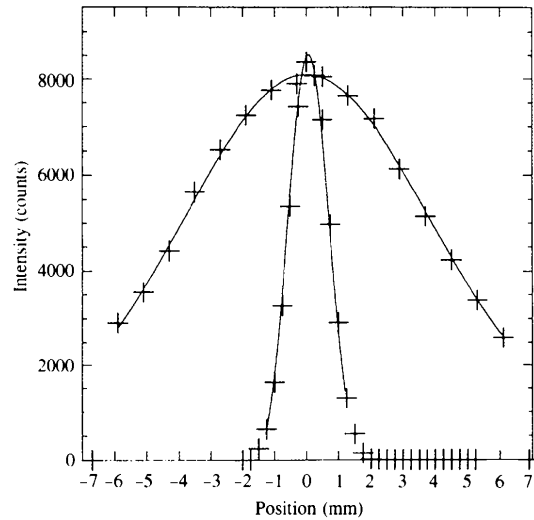


**Figure 5**
Scan of the horizontal and vertical beam size at a distance of 106 m from the undulator for an undulator gap of 20 mm, with PETRA operating at 12 GeV with an emittance of 52 nm rad horizontal and 1.4 nm rad vertical. The solid lines are Gaussian fits through the experimental data points.

tances of 1.4 and 2 nm rad and a $0.25 \times 0.25$ mm$^2$ pinhole at a distance of 106 m. The result was convoluted with the Si(Li) detector response function and Compton profile broadening function. The detector response function can be described as a Gaussian, with an FWHM of $(N^2 + 2.355^2 \omega FE)^{1/2}$, where $N$ corresponds to the electronics noise, $\omega$ is the energy for electron–hole pair production, $F$ is the Fano factor, and $E$ the incident photon energy. The values for the electronic noise of $N = 233$ eV and the Fano factor of $F = 0.129$ were obtained from Si(Li) detector calibration runs in the 8–50 keV energy range. The Compton profile broadening function is described as a Gaussian, with an FWHM of $0.0147E$. The energy broadening due to the finite acceptance of the detector, the
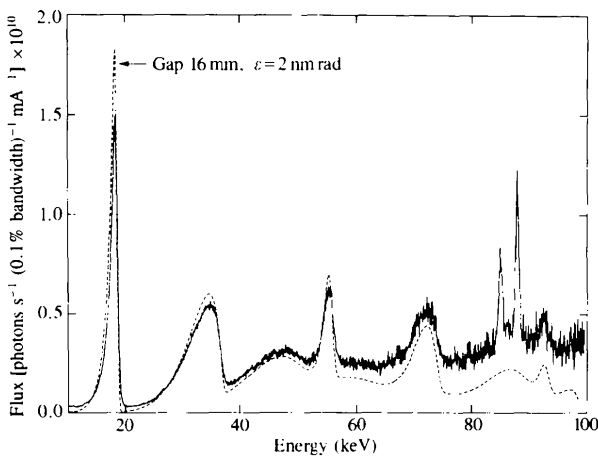
scattering angle, and energy spread of the electrons were small compared with the FWHM of the detector response function and Compton profile broadening, and thus were not included in the calculation.

In Figs. 6–8 the agreement for the first harmonic is ~81% for gaps of 16 and 20 mm and 91% for the 24 mm gap. This is a very satisfying result for an absolute flux measurement and can be further improved by reducing some of the uncertainties listed below. The accuracy of the flux measurements for the energy range below 60 keV was estimated to be ~30%. This includes the following uncertainties:

(i) ~8% attributed to the slit sizes and alignment of slits;

(ii) ~9% in defining the number of He atoms which scatter photons in the detector (scattering geometry, helium pressure and temperature);

(iii) ~10% in estimating the detector efficiency (without radial dependence);

(iv) 1–5% statistical error.

For the energy range above 60 keV the measurements are less reliable. The entrance slit becomes partly transmitting, the detector efficiency decreases, and the background from random scattering increases. The accuracy of measurements with this experimental set-up was further improved during an undulator diagnostic run at APS (Cai et al., 1996).

**Figure 6**

On-axis undulator spectral flux at a gap size of 16 mm through a $0.25 \times 0.25$ mm$^2$ pinhole at 106 m. Solid line: experimental; dashed line: calculated and convoluted with the Si(Li) detector response function and Compton profile broadening.
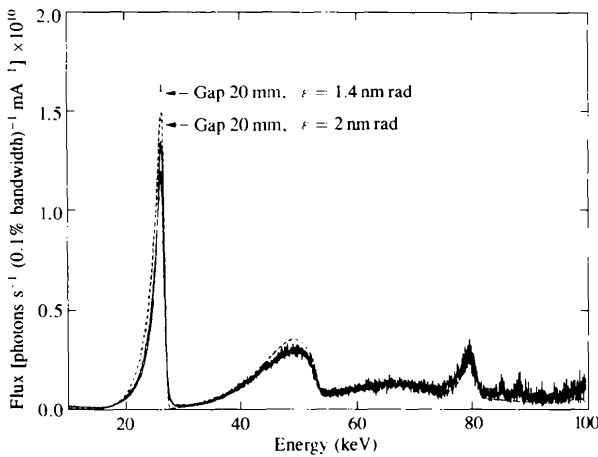


**Figure 7**

On-axis undulator spectral flux at a gap size of 20 mm through a $0.25 \times 0.25$ mm$^2$ pinhole at 106 m. The additional measurement shows the intensity distribution with improved emittance ($\varepsilon = 1.4$ nm rad). Solid line: experimental; dashed line: calculated and convoluted with the Si(Li) detector response function and Compton profile broadening.
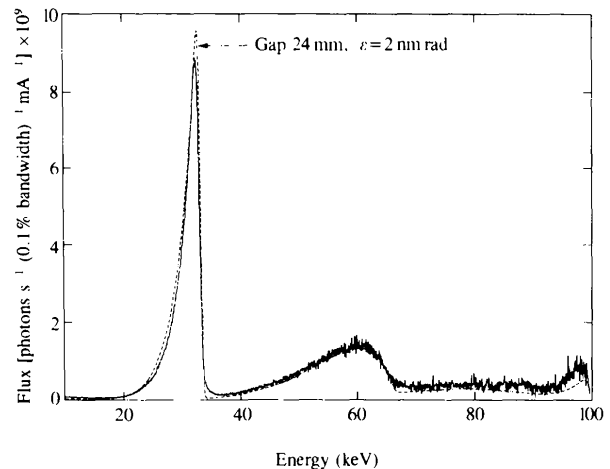


Energy (keV)

**Figure 8**

On-axis undulator spectral flux at a gap size of 24 mm through a $0.25 \times 0.25$ mm$^2$ pinhole at 106 m. Solid line: experimental; dashed line: calculated and convoluted with the Si(Li) detector response function and Compton profile broadening.

## References

Balewski, K., Brefeld, W., Hahn, U., Pflüger, J. & Rossmanith, R. (1995). *Proceedings of the 16th International Conference on High Energy Accelerators, Dallas, Texas, USA.* Vol. 1, p. 275. Piscataway, NJ: APS/IEEE.

Barraza, J., Shu, D. & Kuzay, T. M. (1994). *Nucl. Instrum. Methods,* A**347**, 591–597.

Cai, Z., Dejus, R., Den Hartog, P., Feng, Y., Gluskin, E., Haeffner, D., Ilinski, P., Lai, B., Legnini, D., Moog, E. R., Shastri, S., Trakhtenberg, E., Vassermann, I. & Yun, W. (1996). *Rev. Sci. Instrum.* **67**(9) (CD-ROM).

Cohen, D. D. (1980). *Nucl. Instrum. Methods,* **178**, 481.

HASYLAB (1994*a*). Annual Report, pp. 110–114. HASYLAB, Hamburg, Germany.

HASYLAB (1994*b*). Annual Report, pp. 114–120. HASYLAB, Hamburg, Germany.

Ilinski, P., Yun, W., Lai, B., Gluskin, E. & Cai, Z. (1995). *Rev. Sci. Instrum.* **66**, 1907.